PROCEEDINGS A

royalsocietypublishing.org/journal/rspa

Research

Cite this article: Gautam K, Narayana PAL. 2019 On the stability of carbon sequestration in an anisotropic horizontal porous layer with a first-order chemical reaction. *Proc. R. Soc. A* **475**: 20180365.
http://dx.doi.org/10.1098/rspa.2018.0365

Received: 6 June 2018
Accepted: 9 May 2019

Subject Areas:
applied mathematics, mechanical engineering

Keywords:
anisotropic porous media, carbon sequestration, chemical reaction, stability theory

Author for correspondence:
P. A. L. Narayana
e-mail: ananth@iith.ac.in

On the stability of carbon sequestration in an anisotropic horizontal porous layer with a first-order chemical reaction

K. Gautam and P. A. L. Narayana

Department of Mathematics, Indian Institute of Technology-Hyderabad, Kandi, Sangareddy, Telangana 502285, India

PALN, 0000-0002-1960-0247

Carbon dioxide (CO_2) sequestration in deep saline aquifers is considered to be one of the most promising solutions to reduce the amount of greenhouse gases in the atmosphere. As the concentration of dissolved CO_2 increases in unsaturated brine, the density increases and the system may ultimately become unstable, and it may initiate convection. In this article, we study the stability of convection in an anisotropic horizontal porous layer, where the solute is assumed to decay via a first-order chemical reaction. We perform linear and nonlinear stability analyses based on the steady-state concentration field to assess neutral stability curves as a function of the anisotropy ratio, Damköhler number and Rayleigh number. We show that anisotropy in permeability and solutal diffusivity play an important role in convective instability. It is shown that when solutal horizontal diffusivity is larger than the vertical diffusivity, varying the ratio of vertical to horizontal permeabilities does not significantly affect the behaviour of instability. It is also noted that, when horizontal permeability is higher than the vertical permeability, varying the ratio of vertical to horizontal solutal diffusivity does have a substantial effect on the instability of the system when the reaction rate is dominated by the diffusion rate. We used the Chebyshev-tau method coupled with the QZ algorithm to solve the eigenvalue problem obtained from both the linear and nonlinear stability theories.

1. Introduction

It is well known that the gradual increment in the Earth's temperature is due to the global emissions

THE ROYAL SOCIETY PUBLISHING

of anthropogenic greenhouse gases, especially carbon dioxide (CO_2), in the Earth's atmosphere. The amount of CO_2 has increased rapidly over the last three decades, which has led to ocean acidification and global climate change with severe potential consequences for human society and nature [1–3].

Carbon capture and storage (CCS) technology is one of the most promising options for reducing anthropogenic CO_2 emissions into the atmosphere by storing it in geological sites [4–6], and it is receiving increased attention [7]. Under thermodynamic conditions, captured CO_2 is injected into underground deep saline aquifers. Upon injection of CO_2 into the deep saline aquifers, the density of supercritical CO_2 is lower than that of the brine, which causes the CO_2 to rise above the brine under the impermeable cap-rock.

Weir *et al.* [8,9] first proposed that, during the storage of CO_2 in a subsurface formation, the dissolution of free-phase CO_2 gas into the aqueous phase increases brine density and the same has been concluded in [10–12]. Since the denser CO_2-enriched brine is now overlying unsaturated brine, this leads to a buoyancy-driven convective instability after some time. Consequently, the denser CO_2-saturated brine is propagated downward in the form of fingers into the unsaturated brine. Density-driven convective instability is a favourable process for injected CO_2 in an aqueous phase, which accelerates the dissolution rate and convective mixing and reduces the time available for safe storage of CO_2 in saline aquifers [11,13].

The density-driven convection in the above process [14] is analogous to temperature-driven Rayleigh–Benard convection in porous media, which was first studied independently by Horton & Rogers [15] and Lapwood [16]. Their investigations led to the conclusion that the onset of convection takes place at the critical thermal Rayleigh number $4\pi^2$.

In this study, we consider the first-order chemical reaction which plays a vital role in convective mixing. Many researchers have studied analytically and numerically the effect of geochemical reactions with convective mixing of dissolved CO_2 in deep saline aquifers. Geochemical reactions affect the concentration of other dissolved species, which leads to a change in density. The density profile then becomes unstable and leads to convective flow, which accelerates the dissolution of CO_2 as first noted in [17] and later confirmed by other researchers [18–26]. Ghesmat *et al.* [22] studied the effect of chemical reaction on the buoyancy-driven phenomena in a porous medium and concluded that, when the Damköhler number is small, the effect of the chemical reaction is negligible. Several researchers have attempted to investigate the effect of different parameters on the stability of dissolution-driven convection in a brine-saturated porous medium by linear instability theory and numerical simulations [11,14,19,21,27–30].

Hill & Morad [14] studied the convective stability analysis in an anisotropic porous medium by considering the steady state in the presence of a first-order chemical reaction. They discovered that varying the ratio of the horizontal to vertical solutal diffusivities did not significantly affect the behaviour of instability. However, when the diffusion rate dominates the solute reaction rate, a change in permeability has a substantial effect on the instability.

Rossa *et al.* [29] studied the effect of hydrodynamic dispersion on the development of convective instabilities in the presence of a first-order reaction in porous media. They concluded that hydrodynamic dispersion changes the shape of the bifurcation diagram of convective-enhanced dissolution. Emami-Meybodi [30] extended the analysis of Rossa *et al.* [29] by considering the capillary transition zone in a saturated anisotropic porous medium. Their investigations led to the conclusion that if the geochemical reaction is significantly large then the diffusive boundary layer is unstable in the presence of both the capillary transition zone and hydrodynamic dispersion, and they performed nonlinear simulations which confirmed the prediction of linear stability analysis.

The principal aim of this article is to investigate the effect of anisotropic permeability as well as anisotropic solutal diffusivity by considering a first-order chemical reaction on the density-driven convective stability in a fluid-saturated porous medium. We performed both a linear instability analysis and global stability analysis using the energy functional approach, which helps to bound the region of stability, on the governing system in the context of carbon sequestration. Since all the sedimentary geological formations are essentially in anisotropic forms and generally have a

layered structure, we define the anisotropic permeability parameter as the ratio of the vertical to horizontal permeability (i.e. $\gamma = k_v/k_h$). Here we consider that the horizontal permeability is greater than that of the vertical permeability, which represent real geological applications (i.e. $\gamma < 1$). This problem generalizes the physical situation considered by Hill & Morad [14], in the sense that heterogeneity for the permeability is considered in all directions, whereas only the variation in vertical permeability was considered in Hill & Morad [14].

Firstly, the effect of anisotropic permeability on steady-state thermal convection was studied by Castinel & Combarnous [31] through linear analysis, and later this analysis was extended by Epherre [32] by taking anisotropic thermal diffusivity into account. Kvernvold & Tyvand [33] extended the above linear analysis to a nonlinear stability analysis. They observed that the stability region and Nusselt number depend on the anisotropic parameter and also showed that the impact of the anisotropic parameter on the linear analysis is greater than that on the nonlinear analysis.

There are only a few researchers who have concentrated on the study of solute convection in anisotropic porous media due to anisotropic permeability to identify the occurrence of the onset of convection [11,27,34–38]. Anisotropy in permeability plays a vital role in the onset of convection in the context of the carbon sequestration in deep saline aquifers. Ennis-King *et al.* [11] have studied the effect of anisotropic permeability on the onset of convection using linear and nonlinear stability analyses subject to a rapid change in boundary conditions. They found that the critical time for the onset of convection and critical wavelength becomes larger (i.e. the system becomes unstable) as vertical permeability decreases. However, in the context of carbon sequestration, a chemical reaction occurs between the supercritical CO_2 and a chemical species in porous rocks. This has not been incorporated in Ennis-King *et al.* [11]. In order to account for this effect of the chemical reaction, Andres & Cardoso [23] considered a more realistic situation in which they identify some conditions where a chemical reaction may significantly delay the onset of convection. However, their study was restricted to the situation where the porous medium is homogeneous in nature. In our present study, along with the induced first-order chemical reaction, we considered non-homogeneity in both permeability and solutal diffusivity. This is a further generalization of the earlier situations considered by Hill & Morad [14].

In a similar way, convective stability via linear and global stability analysis of time-dependent density-driven convection in an isotropic porous medium was studied by Xu *et al.* [27]. Their analysis reveals that, when there is an increment in either horizontal or vertical permeability, the system becomes unstable. Cheng *et al.* [34] have also studied the effect of anisotropic permeability on the onset of convection, and they found that their results agree with the results obtained by Xu *et al.* [27]. Their analysis conveys that the base state (which is diffusion) becomes more unstable and solutal convection can occur earlier.

To be more specific about the recent works on anisotropic permeability, Paoli *et al.* [35] have investigated the influence of anisotropic permeability on the onset of convection in a two-dimensional saturated porous medium with the help of numerical simulation. They observed that, for $\gamma < 1$, the vertical convective flux of solute increases significantly and an increase in horizontal permeability makes the system become unstable (i.e. it increases the horizontal velocity gradient of the saturated fluid and in turn enhances the solute vertical transport). Here, the value of $0.25 \leq \gamma \leq 1$ is chosen to be representative of a real geological application [35].

The rest of the article is established as follows: in §2, we give basic equations for the present problem and non-dimensionalize the equations. In §3, we discuss the stability of the system via linear instability analysis (§3a) and global stability analysis (§3b). We obtain the system of the eigenvalue problems for linear analysis (3.1) and (3.2) and nonlinear analysis (3.8)–(3.10) with the corresponding boundary conditions. At the end, we discuss the numerical results in §4.

2. Mathematical formulation of the problem

We consider a simplified saline aquifer which is a homogeneous porous medium and Ω to be a porous layer saturated with brine. The aquifer is assumed to be confined between two horizontal,

infinite parallel impermeable planes. Let $Oxyz$ be a Cartesian frame of reference and $\Omega = \mathbb{R}^2 \times (-d, d)$, $d > 0$. The fluid is assumed to be incompressible, and the fluid motion in the porous layer is assumed to be governed by Darcy's law, such that

$$\nabla \cdot \mathbf{v} = 0 \tag{2.1}$$

and

$$\frac{\mu}{\mathbf{K}}\mathbf{v} = -\nabla P - \mathbf{b}\rho_f g, \tag{2.2}$$

where $\mathbf{v} = (u, v, w)$ is Darcy's velocity vector, μ is the fluid viscosity, P is the pressure, $\mathbf{K}$ is the second-order permeability tensor, g is the acceleration due to gravity, ρ_f is the fluid density and $\mathbf{b} = (0, 0, 1)$. In terms of components, equation (2.2) can be written as

$$\frac{\mu}{k_h}u = -\frac{\partial P}{\partial x}, \tag{2.3}$$

$$\frac{\mu}{k_h}v = -\frac{\partial P}{\partial y} \tag{2.4}$$

and

$$\frac{\mu}{k_v}w = -\frac{\partial P}{\partial z} - \rho_f g, \tag{2.5}$$

where k_h and k_v are the horizontal and vertical permeabilities, respectively, and are assumed to be spatially uniform.

We consider the dissolution of CO_2 in Ω (brine), where the CO_2 undergoes a first-order chemical reaction with brine, and this dissolution of CO_2 increases the density of the brine. When the reaction is introduced, it should be noted that it has a stabilizing effect on the system because it consumes a heavy solute. The transport of CO_2 into brine is governed by the convection–diffusion equation, as is given by [14,28]

$$\phi\frac{\partial C}{\partial t} + \mathbf{v}\cdot\nabla C = \phi D_H \nabla_1^2 C + \phi D_V \frac{\partial^2 C}{\partial z^2} - \beta C, \tag{2.6}$$

where ϕ is the porosity, C is the concentration of CO_2 in brine, β is the reaction rate of CO_2 in brine and D_H and D_V are the horizontal and vertical solutal diffusivities, respectively. The density of the brine ρ_f is affected by the concentration C of CO_2, which is assumed to be linear because the concentration of CO_2 has a very small effect on the partial molar volume [39]. In equation (2.6), we have $\nabla_1^2 = \partial^2/\partial x^2 + \partial^2/\partial y^2$. Further, it is assumed that the linear Boussinesq approximation is valid, which may be written as

$$\rho_f = \rho_0(1 + \beta_c(C - C_0)), \tag{2.7}$$

where ρ_0 is the density of unsaturated brine, C_0 is the reference value of the concentration of CO_2 and β_c is the solutal expansion coefficient.

As we have already assumed that the top and bottom boundaries are impermeable for the fluid flow, we have $\mathbf{v} = 0$ at $z = \pm d$. The upper boundary condition at $z = d$ is assumed to be a constant C_0 and the lower boundary is assumed to be a no-flux condition with the assumption that the dissolved CO_2 cannot escape through the lower boundary, i.e.

$$\frac{\partial C}{\partial z}\Big|_{z=-d} = 0.$$

We now introduce the following scaling for the variables to get the non-dimensional governing equations:

$$x = \frac{d}{\sqrt{\gamma}}x^*, \quad y = \frac{d}{\sqrt{\gamma}}y^*, \quad z = dz^*, \quad C = C_0C^*, \quad t = \frac{d^2}{D_V}t^*$$

and

$$u = \frac{\phi D_V}{\sqrt{\gamma}d}u^*, \quad v = \frac{\phi D_V}{\sqrt{\gamma}d}v^*, \quad w = \frac{\phi D_V}{d}w^*, \quad P = \frac{\phi\mu D_V}{k_v}P^*.$$

Substituting these non-dimensional variables into the governing equations (2.1)–(2.7) and dropping the star, we obtain a non-dimensionalized system of equations in vector form, as

$$\nabla \cdot \mathbf{v} = 0, \tag{2.8}$$

$$\mathbf{v} = -\nabla P - \mathbf{b}\frac{\rho_0 g k_v d}{\phi \mu D_V}(1 + \beta_c C_0(C-1)) \tag{2.9}$$

and

$$\frac{\partial C}{\partial t} + \mathbf{v}\cdot\nabla C = \frac{\partial^2 C}{\partial z^2} + \frac{\gamma}{\eta}\left(\frac{\partial^2 C}{\partial x^2} + \frac{\partial^2 C}{\partial y^2}\right) - \frac{\beta d^2}{\phi D_V} C, \tag{2.10}$$

and the boundary conditions get reduced to

$$\mathbf{v} = 0, \quad C = 1 \quad \text{at } z = 1 \tag{2.11}$$

and

$$\mathbf{v} = 0, \quad \frac{\partial C}{\partial z} = 0 \quad \text{at } z = -1, \tag{2.12}$$

where $\gamma = k_v/k_h$ is the ratio of vertical to horizontal permeabilities and $\eta = D_V/D_H$ is the ratio of vertical to horizontal solutal diffusivities.

We now consider the basic steady-state solution $(\overline{\mathbf{v}}, \overline{P}, \overline{C})$, where the fluid velocity is zero (i.e. $\bar{\mathbf{v}} = 0$) and the concentration field in the base state subject to the boundary conditions is given by

$$\overline{C}(z) = \frac{\cosh\left(\sqrt{d^2\beta_c/\phi D_V}(z+1)\right)}{\cosh\left(2\sqrt{d^2\beta_c/\phi D_V}\right)}. \tag{2.13}$$

To asses the stability analysis, a perturbation $(\mathbf{u}, \pi, \Phi)$ is introduced to the steady-state solution $(\overline{\mathbf{v}}, \overline{P}, \overline{C})$ such that

$$\mathbf{v} = \overline{\mathbf{v}} + \mathbf{u}, \quad P = \overline{P} + \pi \quad \text{and} \quad C = \overline{C} + \Phi.$$

Upon substituting these in the governing equations (2.8)–(2.12), we get the equations for perturbations as

$$\nabla \cdot \mathbf{u} = 0, \tag{2.14}$$

$$\mathbf{u} = -\nabla\pi - \mathbf{b}Ra\Phi \tag{2.15}$$

and

$$\frac{\partial \Phi}{\partial t} + \mathbf{u}.\nabla\Phi + \sqrt{RaDa}M_1(z)w = \frac{\partial^2 \Phi}{\partial z^2} + \frac{\gamma}{\eta}\nabla_1^2\Phi - RaDa\Phi, \tag{2.16}$$

where

$$u_3 = w, \quad \nabla_1^2 = \frac{\partial^2}{\partial x^2} + \frac{\partial^2}{\partial y^2}, \quad M_1(z) = \frac{\sinh\left(\sqrt{RaDa}(z+1)\right)}{\cosh\left(2\sqrt{RaDa}\right)}$$

and

$$Ra = \frac{g\rho_0\beta_c k_v d C_0}{\phi\mu D_V}, \quad Da = \frac{\beta d\mu}{g\rho_0\beta_c C_0 k_v},$$

with Ra and Da being the vertical solutal Rayleigh number and the Damköhler number, respectively. The boundary conditions for perturbations are now

$$w = 0, \quad \Phi = 0 \quad \text{at } z = 1 \tag{2.17}$$

and

$$w = 0, \quad \frac{\partial \Phi}{\partial z} = 0 \quad \text{at } z = -1. \tag{2.18}$$

We assume that the perturbations $(\mathbf{u}, \pi, \Phi)$, defined on $(x, y, z) \in \mathbb{R}^2 \times [-1, 1]$, are periodic functions in the x- and y-directions of periods $2\pi/a_x$ and $2\pi/a_y$, respectively, with $a_x > 0$, $a_y > 0$, being wavenumbers in the x- and y-directions. We shall denote the periodicity cell by $\Omega = [0, 2\pi/a_x] \times [0, 2\pi/a_y] \times [-1, 1]$.

3. Stability analysis

It is crucial to assess the onset of convection (i.e. instability) after dissolution of CO_2 in brine to understand the processes occurring in CO_2 sequestration in saline aquifers. To achieve this, we perform two different stability analyses: namely the linear instability analysis and the nonlinear stability analysis using the energy functional approach [40,41]. The literature reveals that the linear theory gives only a sufficient condition for the instability and nonlinear analysis via the energy functional gives a sufficient condition for the stability of system. The reason for studying both the linear and nonlinear stability analyses is to identify the regions of sub-critical instabilities, if they exist, for the parameter space governing the given flow.

Once we get the eigenvalue problems in both of these theories, we resort to numerical schemes such as the Chebyshev-tau method [42], which is coupled with the QZ algorithm [43], to understand the stability mechanism.

(a) Linear instability analysis

To proceed with the linear instability analysis, it is assumed that the perturbations are too small and so the quadratic and higher order terms (i.e. nonlinear terms) are neglected to get the linearized perturbation equations. This approach provides limited information on the behaviour of the nonlinear system. As the resulting system is linear and autonomous, we may seek solutions of the form

$$[u, v, w, \pi, \Phi] = [u(z), v(z), w(z), \pi(z), \Phi(z)]p_f(x, y)\, e^{\sigma t},$$

where $p_f(x, y) = e^{\mathrm{i}(a_x x + a_y y)}$ is a plan-form which tiles the plane (x, y) with $\nabla_1^2 p_f(x, y) = -a^2 p_f(x, y)$, such that $a^2 = a_x^2 + a_y^2$ (a^2 being the overall wavenumber). The plan-forms represent the horizontal shape of the convection cells formed at the onset of instability. These cells form a regular horizontal pattern tiling the (x, y)-plane, where the wavenumber a is a measure of the width of the convection cell and σ is a growth rate parameter and complex time constant.

Taking the double curl to the linearized version of equation (2.15), where the third component is chosen (i.e. $u_3 = w$ and the fact that $\mathbf{u}$ is solenoidal) and letting $D = \mathrm{d}/\mathrm{dz}$, we derived the following eigenvalue problem for the linear stability analysis:

$$(D^2 - a^2)w - a^2 Ra\Phi = 0 \tag{3.1}$$

and

$$\left(D^2 - a^2\frac{\gamma}{\eta}\right)\Phi - RaDa\Phi - \sqrt{RaDa}M_1(z)w = \sigma\Phi, \tag{3.2}$$

with the boundary conditions $w = 0$, $\Phi = 0$ at $z = 1$ and $w = 0$, $(\partial\Phi/\partial z) = 0$ at $z = -1$.

The fourth-order system (3.1) and (3.2) was solved by using the Chebyshev-tau method [42], which is a spectral technique coupled with the QZ algorithm [43]. We found that the growth rate parameter σ is real at the onset of convection for all governing parameter ranges considered in the present problem. We define the critical value of Ra at the onset as the minimum of Ra with varying a^2 for fixing other flow-governing parameters.

(b) Nonlinear stability analysis

We now try to obtain a bound for global nonlinear stability in the $L^2(\Omega)$ stability measure. To achieve this bound, we first remove the pressure term from the equation (2.15) by taking the double curl on it, to get

$$\nabla^2 w + Ra\left(\frac{\partial^2\Phi}{\partial x^2} + \frac{\partial^2\Phi}{\partial y^2}\right) = 0. \tag{3.3}$$

To proceed with the global stability analysis of convective flow in the porous medium, we use the generalized energy technique by adopting the differential constraints approach

[14,44–46]. Now multiplying equation (2.16) by Φ and integrating over the whole domain Ω using integration by parts and the boundary conditions, we get

$$\frac{1}{2}\frac{\mathrm{d}}{\mathrm{d}t}\|\Phi\|^2 = -\left\|\frac{\partial\Phi}{\partial z}\right\|^2 - \frac{\gamma}{\eta}\|\nabla_1\Phi\|^2 - RaDa\|\Phi\|^2 - \sqrt{RaDa}\langle M_1 w, \Phi\rangle, \tag{3.4}$$

where $\nabla_1 = i\partial/\partial x + j\partial/\partial y$ and $\|.\|$ and $\langle .,.\rangle$ denote the norm and inner product on $L^2(\Omega)$, respectively. Now we define the energy functional E as

$$E(t) = \tfrac{1}{2}\|\Phi\|^2.$$

Differentiating E with respect to t and by using equation (3.4), we derive the following identity:

$$\frac{\mathrm{d}E}{\mathrm{d}t} = \mathcal{I} - \mathcal{D},$$

where

$$\mathcal{I} = -\sqrt{RaDa}\langle M_1 w, \Phi\rangle \tag{3.5}$$

and

$$\mathcal{D} = \left\|\frac{\partial\Phi}{\partial z}\right\|^2 + \frac{\gamma}{\eta}\|\nabla_1\Phi\|^2 + RaDa\|\Phi\|^2. \tag{3.6}$$

We now define the maximization problem as $(1/R_E) = \max_{\mathcal{H}}\mathcal{I}/\mathcal{D}$, where $\mathcal{H}$ is the space of admissible perturbations to equations (2.14)–(2.16) subject to constraint equation (3.3). Now using the Poincaré inequality, it follows that $\mathcal{D} \geq rE$ for some positive constant r, such that

$$\frac{\mathrm{d}E}{\mathrm{d}t} \leq -\left(1 - \frac{1}{R_E}\right) rE.$$

After integration, we have $E(t) \leq E(0)\, e^{-\alpha t}$, $\alpha = r(1 - (1/R_E))$. If $R_E > 1$, then $E(t) \to 0$ as $t \to \infty$. By the definition of $E(t)$, it is clear that the perturbation Φ decays to zero as $t \to \infty$.

However, for the global nonlinear stability, all perturbations must decay to zero (i.e. the decay of $\mathbf{u}$ must also be demonstrated). Multiplying equation (2.15) by $\mathbf{u}$ and integrating over Ω and by using the Cauchy–Schwartz and Young inequalities, we get

$$\|\mathbf{u}\|^2 \leq Ra\left(\frac{\vartheta}{2}\|\Phi\|^2 + \frac{1}{2\vartheta}\|\mathbf{u}\|^2\right), \tag{3.7}$$

for constant $\vartheta > 0$. By choosing the constant $\vartheta = Ra$, we derive

$$\|\mathbf{u}\|^2 \leq Ra^2\|\Phi\|^2.$$

As $\Phi \to 0$, by the definition of $E(t)$ in the stability measure $L^2(\Omega)$ as $t \to \infty$, it clearly shows the decay of $\mathbf{u}$. We now introduce the Euler–Lagrange multiplier τ such that

$$\tau(\mathbf{x})\left[\nabla^2 w + Ra\left(\frac{\partial^2\Phi}{\partial x^2} + \frac{\partial^2\Phi}{\partial y^2}\right)\right] = 0.$$

The Euler–Lagrange equations for the maximization problem $1/R_E$ are now derived and these are subject to normal modes as given in section 3a, to get

$$R_E((D^2 - a^2)w - a^2 Ra\Phi) = 0, \tag{3.8}$$

$$R_E\left((D^2 - a^2)\tau - \sqrt{RaDa}M_1\Phi\right) = 0 \tag{3.9}$$

and

$$R_E\left(\sqrt{RaDa}M_1 w + a^2 Ra\tau\right) = 2\left(D^2 - a^2\frac{\gamma}{\eta}\right)\Phi - 2RaDa\Phi. \tag{3.10}$$

And the boundary conditions get reduced to

$$w = 0, \quad \tau = 0, \quad \Phi = 0 \quad \text{at } z = 1 \tag{3.11}$$

and

$$w = 0, \quad \tau = 0, \quad \frac{\partial\Phi}{\partial z} = 0 \quad \text{at } z = -1. \tag{3.12}$$

The above system (3.8)–(3.12) forms a sixth-order eigenvalue problem for R_E, where global stability holds if $R_E > 1$ for all eigenvalues R_E (while maximizing over Ra and minimizing over a^2) and it was numerically solved by using the Chebyshev-tau method [42], which is coupled with the QZ algorithm [43].

4. Results and discussion

In this section, we present the numerical results of the eigenvalue problems derived in both the linear and nonlinear stability theories. For the linear instability results, it is always found that, for the given set of flow-governing parameters, the growth rate parameter σ is real. Since the sedimentary rocks generally have a layered structure, the permeability in the vertical direction is often much less than that in the horizontal direction. The studies of Xu *et al.* [27] and De Paoli *et al.* [35] reveal that the typical values of vertical permeability cannot exceed 1; however, one can have larger values of horizontal permeability. With this restriction, during the numerical experiment, we set the representative value of the permeability ratio parameter between 0.25 and 1.

Figure 1 gives the variation of critical Ra against Da with varying η for fixed $\gamma = 0.5$. From this figure, it is observed that the behaviour of neutral stability curves for each value of η follow the same trend for either isotropic or anisotropic permeability in the medium. It is noted that an increase in the value of η reduces the value of the critical Rayleigh number, which makes the system unstable. This is clear from the scaling used for η and Ra—that η is linearly proportional to the vertical diffusivity D_V in the medium, whereas Ra is inversely proportional to D_V. Here it is noted that increasing the value of Da up to 0.05 (i.e. in the region where the reaction rate is much smaller than the diffusion rate) the threshold for onset of convection is decreased, clearly indicating the instability in the system; this implies that the penetration of dissolved CO_2 inside resident brine becomes very fast (i.e. convective mixing occurs), and thereafter increasing Da beyond 0.05 the system is stabilized where now the reaction is comparatively stronger than the diffusion rate. It is noted in Hill & Morad [14] that, for varying $\log(Da)$, an increment in the solutal diffusivity ratio increases the solutal Rayleigh number and hence a stabilization is seen for smaller values of the vertical permeability parameter. In our case, we observed that increasing the diffusivity ratio parameter, η, has a destabilization effect. However, we conclude that our results are in line with those of Hill & Morad [14] as the diffusivity ratio parameter defined in the present article is exactly the reciprocal of the diffusivity ratio parameter defined in their article.

Figure 2 gives a visual representation of the linear instability threshold for the variety of γ for a fixed value of $\eta = 0.5$. It is clear from this figure that the behaviour of the neutral stability curves for each value of γ follows a similar pattern when the horizontal solutal diffusion is more than the vertical solutal diffusion. It is noted that an increment in the value of γ (i.e. horizontal permeability is much less than vertical permeability) makes the system stable (varying the ratio of horizontal to vertical permeability does not significantly affect the behaviour of instability). What is to be noted is that increasing the value of Da up to 0.05 (i.e. in the region where the reaction rate is much smaller than the diffusion rate) the threshold for the onset of convection is decreased, clearly indicating the instability in the system. Thereafter increasing Da beyond 0.05 stabilizes the system where the reaction rate is comparatively dominant. Stability of the system does not imply a reduction in trapping of CO_2 in saline aquifers but instability in the system instigates the onset of convection and favours convective mixing.

Figure 3 gives the variation of critical Ra against γ with varying Da for fixed $\eta = 1$. From this figure, it is observed that an increase in γ (i.e. vertical permeability dominates horizontal permeability) stabilizes the system, and this is expected as Ra is linearly proportional to the vertical permeability. The critical value of Ra is reduced by increasing Da in the interval (0.0005, 0.01) as the solutal diffusion rate dominates the chemical reaction rate in the region where the horizontal permeability is high compared with the vertical permeability. On the other hand, for the case where the chemical reaction rate is more dominant than the solutal diffusion rate, it is noted that increasing the value of Da from 0.1 onwards the critical value of Ra is increased and

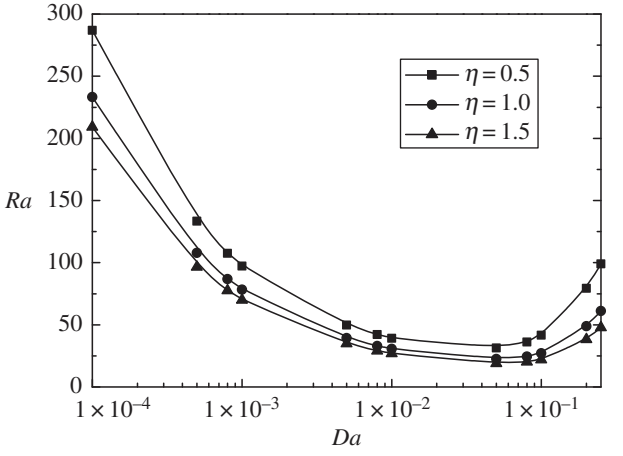

Figure 1. Visual representation of the linear instability threshold for $\eta = 0.5$, 1.0 and 1.5 with the critical solutal Rayleigh number *Ra* plotted against *Da*, where $\gamma = 0.5$.

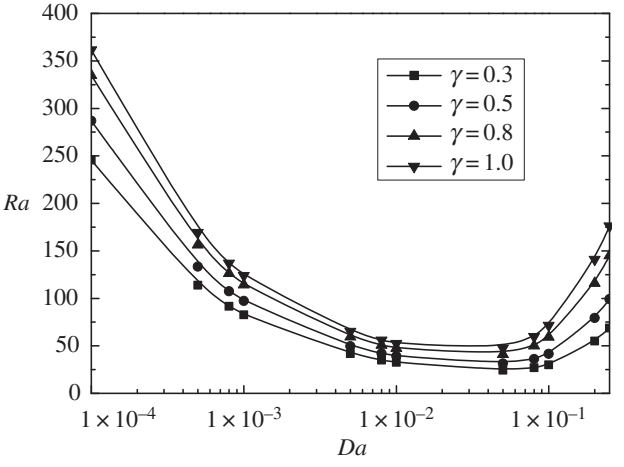

Figure 2. Visual representation of the linear instability threshold for $\gamma = 0.3$, 0.5, 0.8 and 1.0 with the critical solutal Rayleigh number *Ra* plotted against *Da*, where $\eta = 0.5$.

stabilization is seen. This shows that higher values of *Da* show a stabilizing effect with increasing permeability ratio. It has been shown that the chemical reaction between dissolved CO_2 and a solid porous matrix delays the onset of convection in the theoretical works by Ennis-King & Paterson [20], Ghesmat *et al.* [22] and Andres & Cardoso [24]. From figure 3, it is observed that when $Da \ll 1$ (diffusion dominates reaction rate) there is no significant effect of chemical reaction on the stability of the system. However, increasing the vertical permeability increases the critical value of *Ra* at the onset between dissolved CO_2 and the solid porous matrix. In figures 2 and 3, we fixed the γ-values between 0.25 and 1, since the sedimentary rocks generally have a layered structure and the permeability in the vertical direction is often much less than the permeability in the horizontal direction. Even if γ is increased further, the critical value of *Ra* at the onset will increase and the flow gets stabilized.

When the porous medium is homogeneous, Andres & Cardoso [23] pointed out that there exists a critical value of Da/Ra^2, after which the flow is stabilized. This clearly suggests that, when the reaction rate dominates, the flow can withstand the disturbances and the convective mixing between supercritical CO_2 and the brine gets delayed. Exactly the same kind of observation

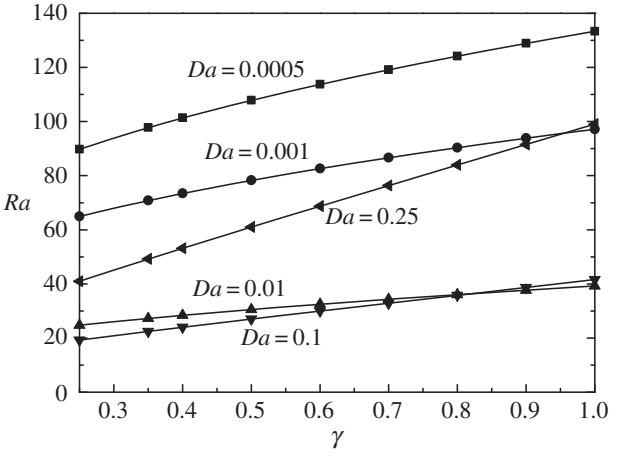

Figure 3. Visual representation of the linear instability threshold for $Da = 0.0005$, 0.001, 0.01, 0.1 and 0.25 with the critical solutal Rayleigh number Ra plotted against γ, where $\eta = 1$.

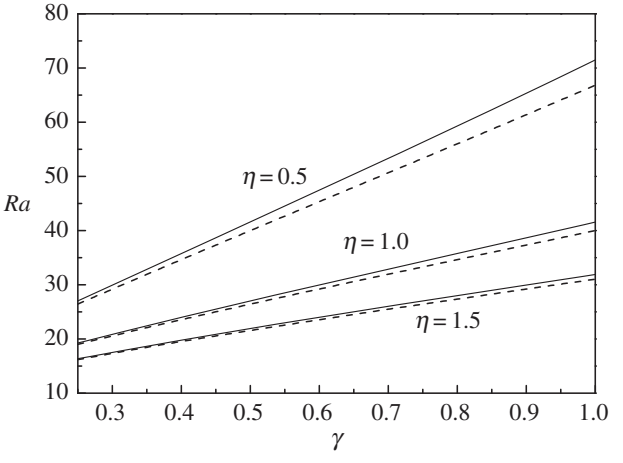

Figure 4. Visual representation of the linear instability (solid lines) and nonlinear stability (dashed lines) threshold for $\eta = 0.5$, 1.0 and 1.5 with the critical solutal Rayleigh number Ra plotted against γ, where $Da = 0.1$.

is made in our results even in the presence of anisotropy with respect to both permeability and solutal diffusivity in the medium. As a consequence, we can conclude that our results in an anisotropic porous medium are in line with the results of Andres & Cardoso [23] in the homogeneous porous case.

The threshold values of Ra in both linear and nonlinear theories against γ with varying η and for varying Da are shown in figures 4 and 5. In these graphs, the solid lines represent the linear stability results and the dashed lines represent the nonlinear stability results. From figure 4, it is to be noted that varying γ increases the threshold values of the onset of convection in both the linear and nonlinear theories and thereby favours the stability, whereas increasing the value of η reduces the critical value of Ra in both the linear and nonlinear theories. Hence η has a destabilizing effect on the system, which is also observed in figure 1. It is further noted that both the linear and nonlinear stability thresholds coincide for smaller values of γ, but as the value of γ is increased the gap between these two theories increases. This confirms that γ is a potential candidate to generate sub-critical instabilities in the medium (i.e. higher vertical permeability can

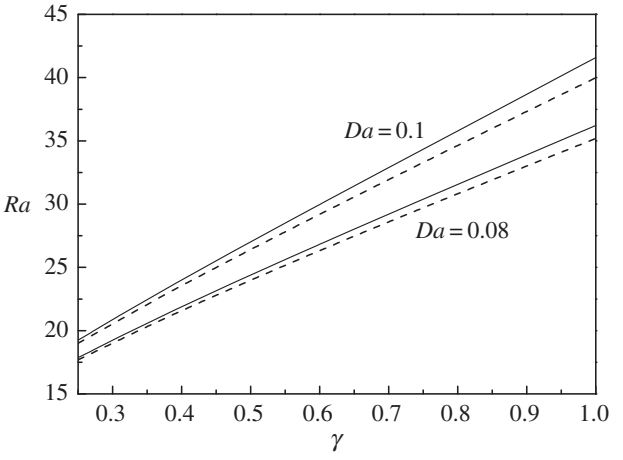

Figure 5. Visual representation of the linear instability (solid lines) and nonlinear stability (dotted lines) threshold for $Da = 0.08$ and 0.1 with the critical solutal Rayleigh number Ra plotted against γ, where $\eta = 1$.

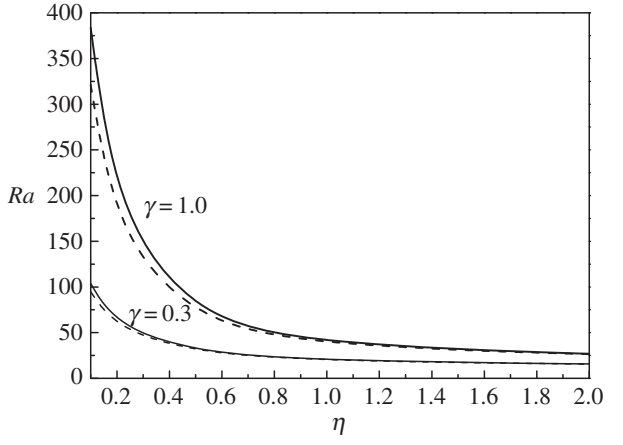

Figure 6. Visual representation of the linear instability (solid lines) and nonlinear stability (dashed lines) threshold for $\gamma = 0.3$ and 1.0 with the critical solutal Rayleigh number Ra plotted against η, where $Da = 0.1$.

cause sub-critical instability), whereas the parameter η has the completely opposite effect on this phenomenon. In other words increasing η reduces the region of sub-critical instabilities. From figure 5, it is observed that varying γ has precisely the same impact on the stability thresholds as discussed in the previous case, but Da plays a stabilizing effect on the system in the region where chemical reaction is dominant. Also, the region of sub-critical instabilities is widened with increasing Da. In conclusion, for a fixed value of γ, it is observed that η and Da have precisely opposite effects on the stability of the system as well as on the region of sub-critical instabilities.

In figure 6, the response of Ra against η is shown for varying γ for fixed $Da = 0.1$, where the reaction dominates diffusion in the medium for both linear and nonlinear theories. For smaller values of η up to 0.5, increasing the γ increases the region of the sub-critical instabilities. In addition, this region of sub-critical instabilities is narrowed with increasing η and after a certain stage both the linear and nonlinear stability thresholds coincide and hence, for higher values of η, linear stability analysis alone is capable of predicting the onset of convection. When vertical solutal diffusion is higher than the horizontal solutal diffusion, both linear and nonlinear

thresholds at the onset of convection coincide and yield no sub-critical region of instability. However, for the case where horizontal solutal diffusion is more than that of vertical solutal diffusion, an increase in the vertical permeability yields the region of sub-critical instabilities.

It is natural to expect a higher value of vertical permeability k_v to enhance fluid motion, and hence favour instability as it consumes more solute, and a higher value of vertical diffusivity to have a stabilizing effect on the system because it reduces the concentration gradients, and hence density gradients. However, in the present analysis, we observe a reverse pattern in the regime diagrams. This is due to the scaling used in §2. When we redefine Ra and Da as $(Ra_m\gamma/\eta)$ and (Da_m/η), respectively (where $Ra_m = (g\rho_0\beta_c k_h d C_0/\phi\mu D_H)$ and $Da_m = (\beta d\mu/g\rho_0\beta_c C_0 k_h)$), we do confirm the expected phenomenon (i.e. increasing k_v decreases the value of Ra_m and as a consequence destabilization is recovered). With this observation, we confirm that the numerical results presented in the problem are correct and validate the physical phenomenon which is already available in the literature. This is because the entire scaling is done using k_v and D_V in the paper while in the literature scaling is performed using k_h and D_H [27,36,37]. This is why our numerical results show a reverse trend to the known results in the literature.

When the permeability ratio γ to diffusivity ratio η is less than 1, the threshold value for onset is less than the threshold value of Ra for $\gamma/\eta > 1$. In general, we cannot predict a particular value of the permeability and diffusivity ratio because anisotropy in permeability depends on the rock structure, which changes from place to place. From this analysis, we can suggest that carbon sequestration system will be more stable with increasing permeability ratio and will be unstable with increasing diffusivity ratio, leading to faster CO_2 dissolution into the brine.

Data accessibility. This article has no additional data.

Authors' contributions. K.G. performed major calculations and simulations. P.A.L.N. contributed towards interpreting the results and corrected the paper several times. Both authors formulated this problem and also gave their final approval for publication.

Competing interests. We declare we have no competing interests.

Funding. K.G. acknowledges the research fellowship provided by the Council of Scientific and Industrial Research (CSIR), Government of India, through grant no. '09/1001(0022)/2016-EMR-I' and the hospitality of the Indian Institute of Technology Hyderabad.

Acknowledgements. We convey our sincere gratitude to the anonymous referees for their constructive criticism and suggestions, which have helped us to improve the paper.

References

1. Holloway S. 2001 Storage of fossil fuel-derived carbon dioxide beneath the surface of the earth. *Annu. Rev. Energy Env.* **26**, 145–166. (doi:10.1146/annurev.energy.26.1.145)
2. Bachu S, Adams JJ. 2003 Sequestration of CO_2 in geological media in response to climate change: capacity of deep saline aquifers to sequester CO_2 in solution. *Energy Convers. Manage.* **44**, 3151–3175. (doi:10.1016/S0196-8904(03)00101-8)
3. Intergovernmental Panel on Climate Change. 2013 *Climate change 2013: the physical science basis*. Geneva, Switzerland: IPCC.
4. Hitchon B, Gunter WD, Gentzis T, Bailey RT. 1999 Sedimentary basins and greenhouse gases: a serendipitous association. *Energy Convers. Manage.* **40**, 825–843. (doi:10.1016/S0196-8904(98)00146-0)
5. Allen DE, Strazisar BR, Soong Y, Hedges SW. 2005 Modeling carbon dioxide sequestration in saline aquifers: significance of elevated pressures and salinities. *Fuel Process. Technol.* **86**, 1569–1580. (doi:10.1016/j.fuproc.2005.01.004)
6. Benson SM, Cole DR. 2008 CO_2 sequestration in deep sedimentary formations. *Elements* **4**, 325–331. (doi:10.2113/gselements.4.5.325)
7. Metz B, Davidson O, De Coninck HC, Loos M, Meyer LA. 2005 *IPCC: Intergovernmental Panel on Climate Change special report on carbon dioxide capture and storage*. Cambridge, UK: Cambridge University Press.
8. Weir GJ, White SP, Kissling WM. 1995 Reservoir storage and containment of greenhouse gases. *Energy Convers. Manage.* **36**, 531–534. (doi:10.1016/0196-8904(95)00060-Q)

9. Weir GJ, White SP, Kissling WM. 1996 Reservoir storage and containment of greenhouse gases. *Transp. Porous Media* **23**, 37–60. (doi:10.1007/bf00145265)
10. Song Y, Nishio M, Chen B, Someya S, Uchida T, Akai M. 2002 Measurement of the density of CO_2 solution by Mach-Zehnder interferometry. *Ann. N. Y. Acad. Sci.* **972**, 206–212. (doi:10.1111/nyas.2002.972.issue-1)
11. Ennis-King J, Preston I, Paterson L. 2005 Onset of convection in anisotropic porous media subject to a rapid change in boundary conditions. *Phys. Fluids* **17**, 084107. (doi:10.1063/1.2033911)
12. Pruess K, Zhang K. 2008 *Numerical modeling studies of the dissolution-diffusion-convection processduring* CO_2 *storage in saline aquifers*. Berkeley, CA: Ernest Orlando Lawrence Berkeley National Laboratory.
13. Hassanzadeh H, Pooladi-Darvish M, Keith DW. 2006 Stability of a fluid in a horizontal saturated porous layer: effect of non-linear concentration profile, initial, and boundary conditions. *Transp. Porous Media* **65**, 193–211. (doi:10.1007/s11242-005-6088-1)
14. Hill AA, Morad MR. 2014 Convective stability of carbon sequestration in anisotropic porous media. *Proc. R. Soc. A* **470**, 20140373. (doi:10.1098/rspa.2014.0373)
15. Horton CW, Rogers Jr FT. 1945 Convection currents in a porous medium. *J. Appl. Phys.* **16**, 367–370. (doi:10.1063/1.1707601)
16. Lapwood ER. 1948 Convection of a fluid in a porous medium. *Math. Proc. Cambridge Philos. Soc.* **44**, 508–521. (doi:10.1017/S030500410002452X)
17. Lindeberg E, Wessel-Berg D. 1997 Vertical convection in an aquifer column under a gas cap of CO_2. *Energy Convers. Manage.* **38**, S229–S234. (doi:10.1016/S0196-8904(96)00274-9)
18. Ennis-King J, Paterson L. 2002 Engineering aspects of geological sequestration of carbon dioxide. In *Proc. SPE Asia Pacific Oil and Gas Conference and Exhibition, Melbourne, Australia, 8–10 October 2002*. Richardson, TX: Society of Petroleum Engineers.
19. Ennis-King JP, Paterson L. 2005 Role of convective mixing in the long-term storage of carbon dioxide in deep saline formations. *SPE J.* **10**, 349–356. (doi:10.2118/84344-PA)
20. Ennis-King J, Paterson L. 2007 Coupling of geochemical reactions and convective mixing in the long-term geological storage of carbon dioxide. *Int. J. Greenhouse Gas Control* **1**, 86–93. (doi:10.1016/S1750-5836(07)00034-5)
21. Riaz A, Hesse M, Tchelepi HA, Orr FM. 2006 Onset of convection in a gravitationally unstable diffusive boundary layer in porous media. *J. Fluid Mech.* **548**, 87–111. (doi:10.1017/S0022112005007494)
22. Ghesmat K, Hassanzadeh H, Abedi J. 2011 The impact of geochemistry on convective mixing in a gravitationally unstable diffusive boundary layer in porous media: CO_2 storage in saline aquifers. *J. Fluid Mech.* **673**, 480–512. (doi:10.1017/S0022112010006282)
23. Andres JTH, Cardoso SS. 2011 Onset of convection in a porous medium in the presence of chemical reaction. *Phys. Rev. E* **83**, 046312. (doi:10.1103/PhysRevE.83.046312)
24. Andres JTH, Cardoso SS. 2012 Convection and reaction in a diffusive boundary layer in a porous medium: nonlinear dynamics. *Chaos: Interdiscip. J. Nonlinear Sci.* **22**, 037113. (doi:10.1063/1.4748866)
25. Kim MC, Choi CK. 2014 Effect of first-order chemical reaction on gravitational instability in a porous medium. *Phys. Rev. E* **90**, 053016. (doi:10.1103/PhysRevE.90.053016)
26. Kim MC, Kim YH. 2015 The effect of chemical reaction on the onset of gravitational instabilities in a fluid saturated within a vertical Hele-Shaw cell: theoretical and numerical studies. *Chem. Eng. Sci.* **134**, 632–647. (doi:10.1016/j.ces.2015.04.020)
27. Xu X, Chen S, Zhang D. 2006 Convective stability analysis of the long-term storage of carbon dioxide in deep saline aquifers. *Adv. Water Res.* **29**, 397–407. (doi:10.1016/j.advwatres.2005.05.008)
28. Ward TJ, Cliffe KA, Jensen OE, Power H. 2014 Dissolution-driven porous-medium convection in the presence of chemical reaction. *J. Fluid Mech.* **747**, 316–349. (doi:10.1017/jfm.2014.149)
29. Rossa GB, Cliffe KA, Power H. 2017 Effects of hydrodynamic dispersion on the stability of buoyancy-driven porous media convection in the presence of first order chemical reaction. *J. Eng. Math.* **103**, 55–76. (doi:10.1007/s10665-016-9860-z)
30. Emami-Meybodi H. 2017 Stability analysis of dissolution-driven convection in porous media. *Phys. Fluids* **29**, 014102. (doi:10.1063/1.4974275)
31. Castinel G, Combarnous M. 1977 Natural convection in an anisotropic porous layer. *Int. Chem. Eng.* **17**, 605–614.

32. Epherre JF. 1977 Criterion for appearance of natural convection in an anisotropic porous layer. *Int. Chem. Eng.* **17**, 615–616.
33. Kvernvold O, Tyvand PA. 1979 Nonlinear thermal convection in anisotropic porous media. *J. Fluid Mech.* **90**, 609–624. (doi:10.1017/S0022112079002445)
34. Cheng P, Bestehorn M, Firoozabadi A. 2012 Effect of permeability anisotropy on buoyancy-driven flow for CO_2 sequestration in saline aquifers. *Water Resour. Res.* **48**, W09539. (doi:10.1029/2012wr011939)
35. De Paoli M, Zonta F, Soldati A. 2016 Influence of anisotropic permeability on convection in porous media: implications for geological CO_2 sequestration. *Phys. Fluids* **28**, 056601. (doi:10.1063/1.4947425)
36. Hong JS, Kim MC. 2008 Effect of anisotropy of porous media on the onset of buoyancy-driven convection. *Transp. Porous Media* **72**, 241–253. (doi:10.1007/s11242-007-9147-y)
37. Rapaka S, Pawar RJ, Stauffer PH, Zhang D, Chen S. 2009 Onset of convection over a transient base-state in anisotropic and layered porous media. *J. Fluid Mech.* **641**, 227–244. (doi:10.1017/S0022112009991479)
38. Green CP, Ennis-King J. 2014 Steady dissolution rate due to convective mixing in anisotropic porous media. *Adv. Water Res.* **73**, 65–73. (doi:10.1016/j.advwatres.2014.07.002)
39. Barbero JA, Hepler LG, McCurdy KG, Tremaine PR. 1983 Thermodynamics of aqueous carbon dioxide and sulfur dioxide: heat capacities, volumes, and the temperature dependence of ionization. *Can. J. Chem.* **61**, 2509–2519. (doi:10.1139/v83-433)
40. Straughan B. 2008 *Stability and wave motion in porous media*. Applied Mathematical Sciences, vol. 165. New York, NY: Springer.
41. Straughan B. 2004 *The energy method, stability, and nonlinear convection*, 2nd edn. Applied Mathematical Sciences, vol. 91. New York, NY: Springer.
42. Dongarra JJ, Straughan B, Walker DW. 1996 Chebyshev tau-QZ algorithm methods for calculating spectra of hydrodynamic stability problems. *Appl. Numer. Math.* **22**, 399–434. (doi:10.1016/S0168-9274(96)00049-9)
43. Straughan B, Walker DW. 1996 Two very accurate and efficient methods for computing eigenvalues and eigenfunctions in porous convection problems. *J. Comput. Phys.* **127**, 128–141. (doi:10.1006/jcph.1996.0163)
44. Pieters GJM, Van-Duijn CJ. 2006 Transient growth in linearly stable gravity-driven flow in porous media. *Eur. J. Mech.-B/Fluids* **25**, 83–94. (doi:10.1016/j.euromechflu.2005.04.008)
45. Hill AA. 2009 A differential constraint approach to obtain global stability for radiation induced double-diffusive convection in a porous medium. *Math. Methods Appl. Sci.* **32**, 914–921. (doi:10.1002/mma.v32:8)
46. Capone F, Gentile M, Hill AA. 2011 Double-diffusive penetrative convection simulated via internal heating in an anisotropic porous layer with throughflow. *Int. J. Heat Mass Transfer* **54**, 1622–1626. (doi:10.1016/j.ijheatmasstransfer.2010.11.020)